Two- and one-photon transitions in a three-level atom inside a cavity with arbitrary damping

G. Adam, J. Seke, and O. Hittmair
Institut für Theoretische Physik, Technische Universität Wien, Wiedner Hauptstrasse 8-10, A-1040 Vienna, Austria
(Received 23 April 1990)

Different aspects of the interaction of a three-level atom with a single-mode radiation field are studied inside a cavity with damping. It is demonstrated that two-photon transitions emerge from cascade one-photon transitions by increasing the detuning parameters of the levels. It is also shown that a simulation of the two-level atom with one-photon transitions can be achieved by changing the detuning parameters adequately. In all cases, the influence of cavity damping is examined. Finally, we point out that the second-order field correlation function approaches its minimum value for $t \to \infty$ in some cases.

I. INTRODUCTION

In the present paper, different aspects of the interaction of a three-level atom with a single-mode radiation field in a cavity with arbitrary damping will be treated. The same model without damping was also investigated by other authors.[1,2] The damping, however, plays a very significant role in experiments since no ideal cavities exist. The importance of the present model is verified by the large number of experiments performed with Rydberg atoms.[3] In this paper the three-level atom model will be used for two different investigations. First of all, the two-photon transition will be demonstrated in the model. Second, it will be shown that the two-level atom can be simulated by a three-level model. Since the inclusion of cavity damping makes the problem so complex that only numerical calculations are possible, we restrict our investigations to the so-called Ξ type of the three-level atom. In our previous paper[4] we presented some preliminary numerical results for the same model in the case of the resonant cavity mode. In the present paper our calculations go into more detail, and the influence of the detuning of the atomic levels will be discussed explicitly. Moreover, new statistical properties, such as antibunching of the radiation field caused by the cavity damping, will be pointed out.

The paper is organized as follows. In Sec. II we set up exact equations of motion for the expectation values (EV's) of interest. In Sec. III we give numerical results for different detunings in the case of two-photon transitions. In Sec. IV the two-level atom will be simulated in the three-level atom model by adequate choice of the level detunings. In Sec. V we study the statistical properties of the field by examining the second-order correlation function. In Sec. VI we draw a conclusion and compare our work with that of other authors[5] who, instead of exact Hamiltonians as in our model, used effective Hamiltonians for description of the two-photon transitions.

II. EQUATIONS OF MOTION FOR EXPECTATION VALUES

Here, we set up equations of motion for the Ξ type of the three-level atom interacting with the single-mode radiation field inside a damped cavity. Furthermore, we restrict ourselves to the one-electron case. The direct transition between level 1 and 3 is not allowed (see Fig. 1). The Liouvillian for our model reads as[1,6-8]

$$LX=[H_{\mathrm{I}}+H_{\mathrm{II}},X]+i\Lambda X\ , \tag{1}$$

where the Hamiltonians[1] H_{I} and H_{II} ($\hbar=1$) are given by

$$H_{\mathrm{I}}=\omega(a^{\dagger}a+b_3^{\dagger}b_3-b_1^{\dagger}b_1)+\omega_2(b_1^{\dagger}b_1+b_2^{\dagger}b_2+b_3^{\dagger}b_3)\ , \tag{2}$$

$$H_{\mathrm{II}}=-\Delta_l b_1^{\dagger}b_1+\Delta_r b_3^{\dagger}b_3+(\xi^{-}ab_2^{\dagger}b_1+\eta^{-}ab_3^{\dagger}b_2+\mathrm{H.c.}) \tag{3}$$

(H.c. denotes the Hermitian conjugates). The cavity

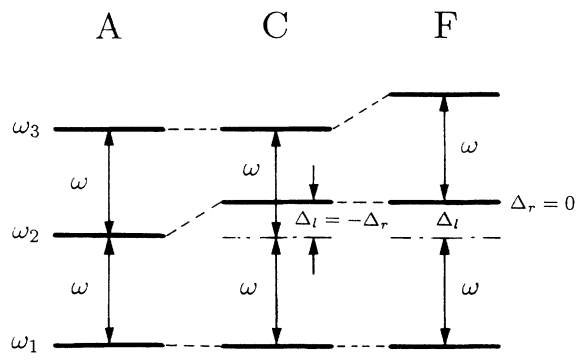

FIG. 1. Different detunings in the cases of the Ξ-type three-level atom [see Eqs. (22)–(27) for case descriptions]. For case A we plot the resonant case without detuning. For case C the detuning parameters are $\Delta_l=-\Delta_r\neq 0$ (exact two-photon resonance). For case F the detuning parameters are chosen so that the transition process simulates a two-level atom ($\Delta_l\neq 0$, $\Delta_r=0$).

damping in Eq. (1) reads as[6-8,9]

$$\Lambda\cdots=\kappa([a\cdots,a^\dagger]+[a,\cdots a^\dagger]) , \tag{4}$$

where κ is the cavity-damping constant. Further, in Eqs. (2)–(4) we used $b_j^\dagger$ and b_j as creation and annihilation operators of an electron at level j, and $a^\dagger$ and a as those of a photon in the single-mode field with frequency ω. The energy levels are denoted by ω_j, $j=1$, 2, and 3, the coupling constants for the transitions $1\rightarrow2$ and $2\rightarrow3$ are given by $\xi^-=(\xi^+)^*$ and $\eta^-=(\eta^+)^*$, respectively, and the detuning parameters are

$$\Delta_l=|\omega_2-\omega_1|-\omega, \quad \Delta_r=|\omega_3-\omega_2|-\omega . \tag{5}$$

For the fermion and boson operators the following commutation relations hold

$$\{b_i,b_j^\dagger\}\equiv b_ib_j^\dagger+b_j^\dagger b_i=\delta_{ij} ,$$
$$\{b_i,b_j\}=0=\{b_i^\dagger,b_j^\dagger\} , \tag{6}$$

$$[a,a^\dagger]\equiv aa^\dagger-a^\dagger a=1, \quad [b_i,a]=0 . \tag{7}$$

In the following we set up the equations of motion for the EV's, for $k=0,1,2,\ldots$:

$$n_k(t)\equiv\mathrm{Tr}[(a^\dagger)^k a^k\rho(t)] \tag{8}$$

$$z_k^i(t)\equiv\mathrm{Tr}\{(a^\dagger)^k a^k b_i^\dagger b_i\rho(t)\}, \quad i=1,2,3 , \tag{9}$$

$$f_k^{i+}(t)\equiv\mathrm{Tr}\{(a^\dagger)^k a^{k+1}b_{i+1}^\dagger b_i\rho(t)\}$$
$$=[f_k^{i-}(t)]^*, \quad i=1,2 , \tag{10}$$

$$d_k^+(t)\equiv\mathrm{Tr}\{(a^\dagger)^k a^{k+2}b_3^\dagger b_1\rho(t)\}=[d_k^-(t)]^* , \tag{11}$$

where $n_1(t)$ is the mean photon number, $z_0^i(t)$, $i=1$, 2, and 3 is the occupation probability of the ith level.

By using the Liouville equation $d\rho/dt=-iL\rho(t)$ for the density operator $\rho(t)$, we obtain a closed set of equations of motion for the EV's, for $k=0,1,2,\cdots$:

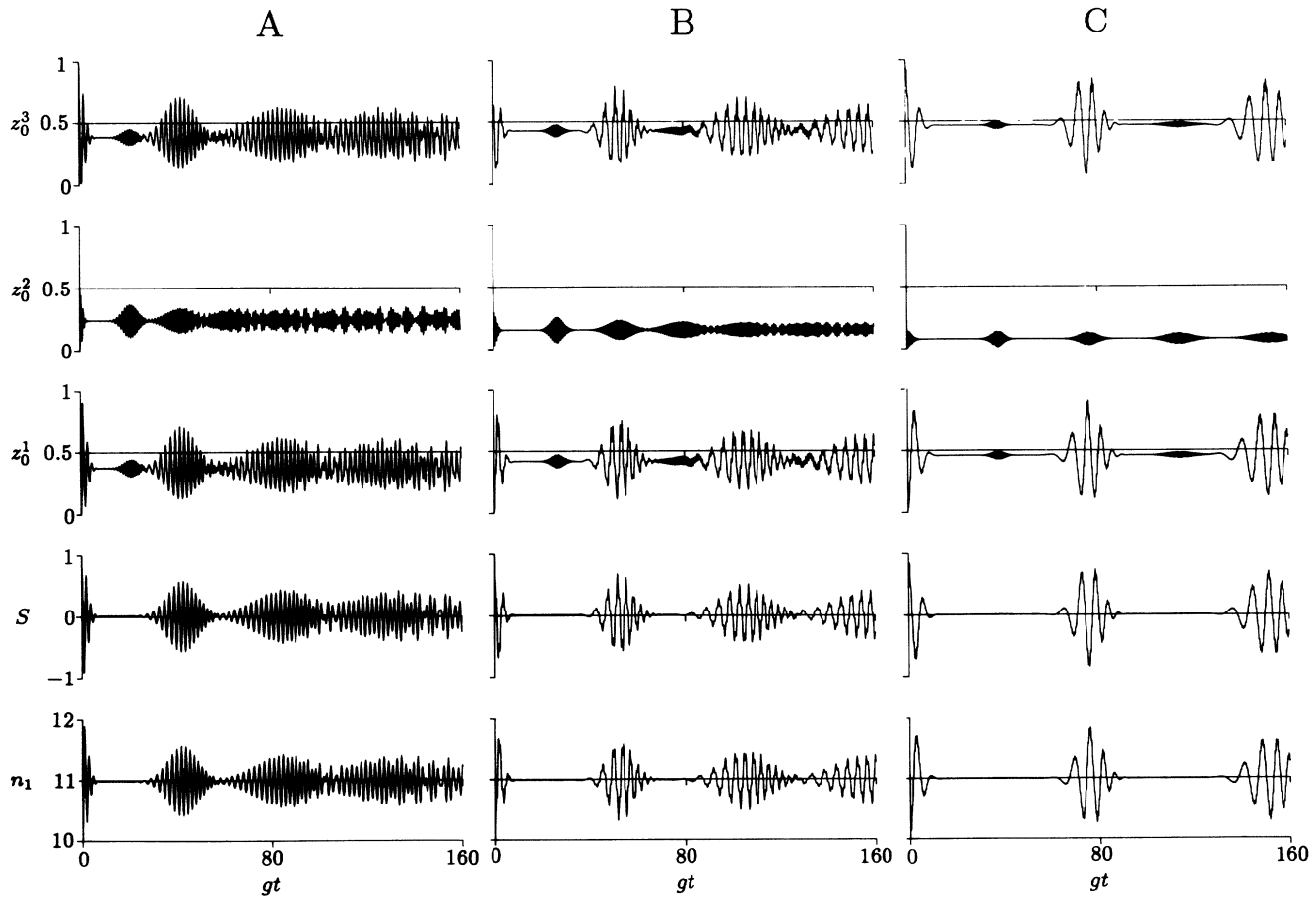

FIG. 2. Atomic-level occupation probabilities $z_0^i(t)$, $i=1$, 2, and 3, occupation inversion $S=z_0^3(t)-z_0^1(t)$ and mean photon number $n_1(t)$ as functions of the scaled time gt, $g=(|\xi^-|^2+|\eta^-|^2)^{1/2}$ for real coupling constants $\xi^-=\eta^-$. The time evolutions are plotted for the resonant Ξ type of the three-level atom in the case of an initial coherent field ($n_1(0)=|\alpha|^2=10$) inside an *ideal cavity* with different detuning parameters: case A, $\Delta_l=-\Delta_r=0$; case B, $\Delta_l=-\Delta_r=5g$; case C, $\Delta_l=-\Delta_r=10g$.

$$\frac{dn_k}{dt} \equiv \dot{n}_k = -2\kappa k n_k + ik(\xi^- f_{k-1}^{1+} + \eta^- f_{k-1}^{2+} - \text{H.c.}) , \tag{12}$$

$$\dot{z}_k^1 = -2\kappa k z_k^1 + i[\xi^-(f_k^{1+} + k f_{k-1}^{1+}) - \text{H.c.}] , \tag{13}$$

$$\dot{z}_k^2 = -2\kappa k z_k^2 + i[-\xi^- f_k^{1+} + \eta^-(f_k^{2+} + k f_{k-1}^{2+}) - \text{H.c.}] , \tag{14}$$

$$\dot{z}_k^3 = -2\kappa k z_k^3 + i(-\eta^- f_k^{2+} - \text{H.c.}) , \tag{15}$$

$$\dot{f}_k^{1\pm} = -(2k+1)\kappa f_k^{1\pm} \pm i\{\xi^{\pm}[z_{k+1}^1 - z_{k+1}^2 - (k+1)z_k^2] + \eta^{\mp}(d_k^{\pm} + k d_{k-1}^{\pm}) + \Delta_l f_k^{1\pm}\} , \tag{16}$$

$$\dot{f}_k^{2\pm} = -(2k+1)\kappa f_k^{2\pm} \pm i\{\eta^{\pm}[z_{k+1}^2 - z_{k+1}^3 - (k+1)z_k^3] - \xi^{\mp} d_k^{\pm} + \Delta_r f_k^{2\pm}\} , \tag{17}$$

$$\dot{d}_k^{\pm} = -(2k+2)\kappa d_k^{\pm} \mp i\{\xi^{\pm}[f_{k+1}^{2\pm} + (k+2)f_k^{2\pm}] - \eta^{\pm} f_{k+1}^{1\pm} - (\Delta_l + \Delta_r) d_k^{\pm}\} . \tag{18}$$

In our calculations we use the initial condition that the atom is in the jth energy level and the field in a coherent state $|\alpha\rangle$, with mean photon number $n_1(0) = \langle a^\dagger a \rangle_0 = |\alpha|^2$:

$$\rho(0) = |j\rangle\langle j| \otimes |\alpha\rangle\langle\alpha| . \tag{19}$$

The initial values of the EV's in Eqs. (12)–(18) for $k = 0, 1, 2, \ldots$ are determined by

$$n_k(0) = |\alpha|^{2k} , \tag{20}$$

$$z_k^i(0) = |\alpha|^{2k}\delta_{ij}, \quad i = 1,2,3, \ldots \tag{21}$$

(the remaining expectation values are zero at the initial time).

The different detuning parameters (for example, see cases A, C, and F in Fig. 1), for which we shall solve the above Eqs. (12)–(18), read as

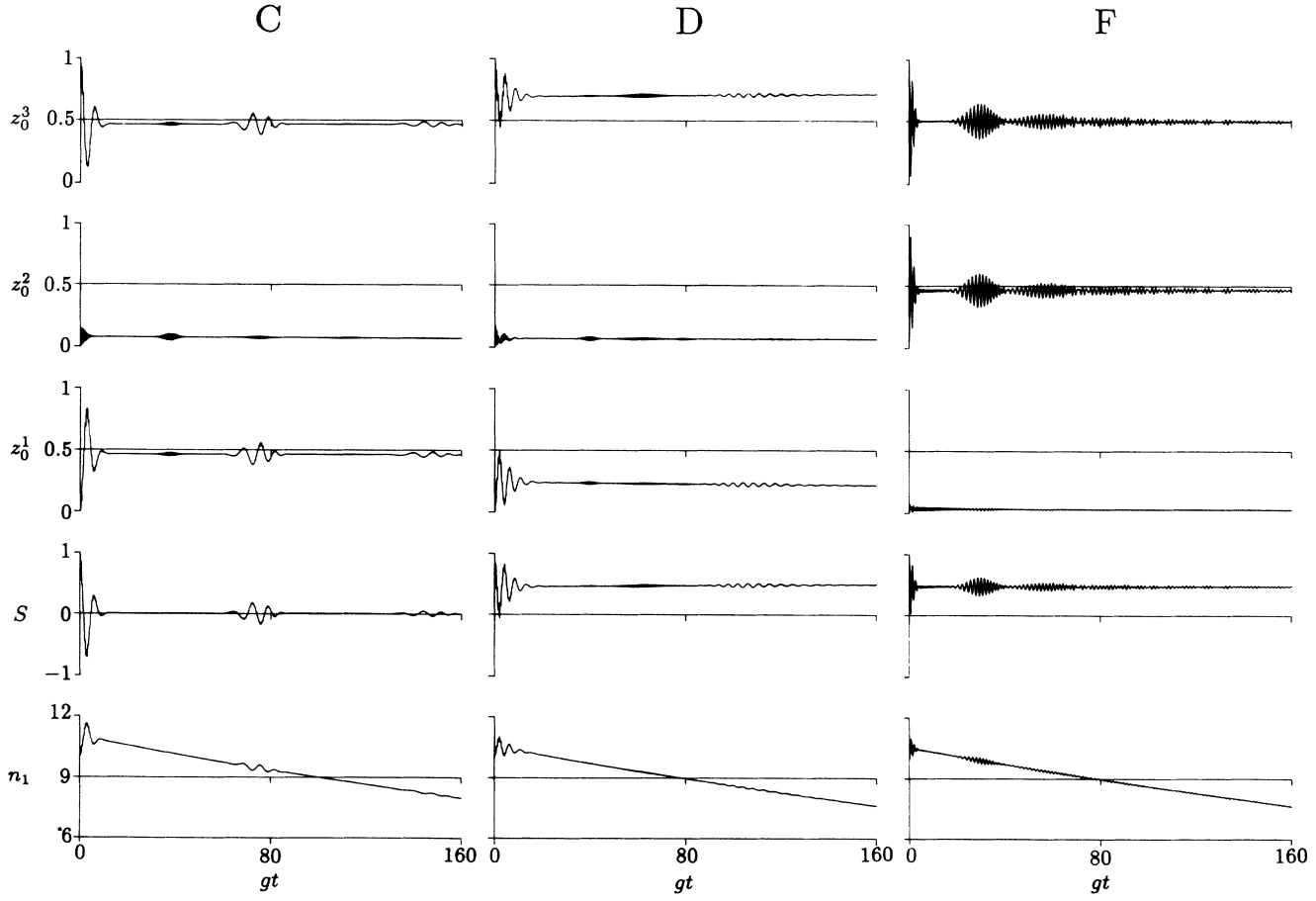

FIG. 3. Same as Fig. 2 for the *cavity with damping*, $\kappa = 0.001g$, and other detuning parameters: case C, $\Delta_l = -\Delta_r = 10g$; case D, $\Delta_l = 10g$, $\Delta_r = -9g$; case F, $\Delta_l = 10g$, $\Delta_r = 0$.

$$\Delta_l=-\Delta_r=0 \text{ for case A}, \tag{22}$$

$$\Delta_l=-\Delta_r=5g \text{ for case B}, \tag{23}$$

$$\Delta_l=-\Delta_r=10g \text{ for case C}, \tag{24}$$

$$\Delta_l=10g,\ \Delta_r=-9g \text{ for case D}, \tag{25}$$

$$\Delta_l=10g,\ \Delta_r=-7g \text{ for case E}, \tag{26}$$

$$\Delta_l=10g,\ \Delta_r=0 \text{ for case F}, \tag{27}$$

where $g=(|\xi^-|^2+|\eta^-|^2)^{1/2}$.

III. NUMERICAL RESULTS FOR DIFFERENT DETUNINGS IN THE CASE OF TWO-PHOTON TRANSITIONS

In this section we solve numerically Eqs. (12)–(18) for the initial conditions (20) and (21), with $j=3$, taking into account the detuning parameters of cases A–F. In Figs. 2–5 we plot the atomic occupation probabilities of the levels $z_0^i(t)$, $i=1$, 2, and 3, the occupation inversion,

$$S(t)=z_0^3(t)-z_0^1(t), \tag{28}$$

and the mean photon number $n_1(t)$.

In Fig. 2 we plot the numerical results for the case of the exact two-photon resonance inside an ideal cavity ($\kappa=0$). The different detuning parameters are given by cases A–C (cf. Fig. 1). From Fig. 2 it can be seen quite clearly that the increasing detuning leads to almost perfect two-photon transitions. The characteristics of the two-photon transition, namely, the almost vanishing occupation probability at intermediate level 2, the long lifetime of the collapses, and the low frequency of the revival oscillations, are clearly exhibited for case C in Fig. 2. In this figure the detuning is increased only to the extent that the influence of the intermediate level 2 is still visible.

In Fig. 3 case C, we explore the influence of weak cavity damping on the two-photon transition. It can be seen that the amplitudes of the revival oscillations decrease as a consequence of the cavity damping, but the significant features of the undamped case are still preserved. The cavity losses are only visible in the pronounced decay of

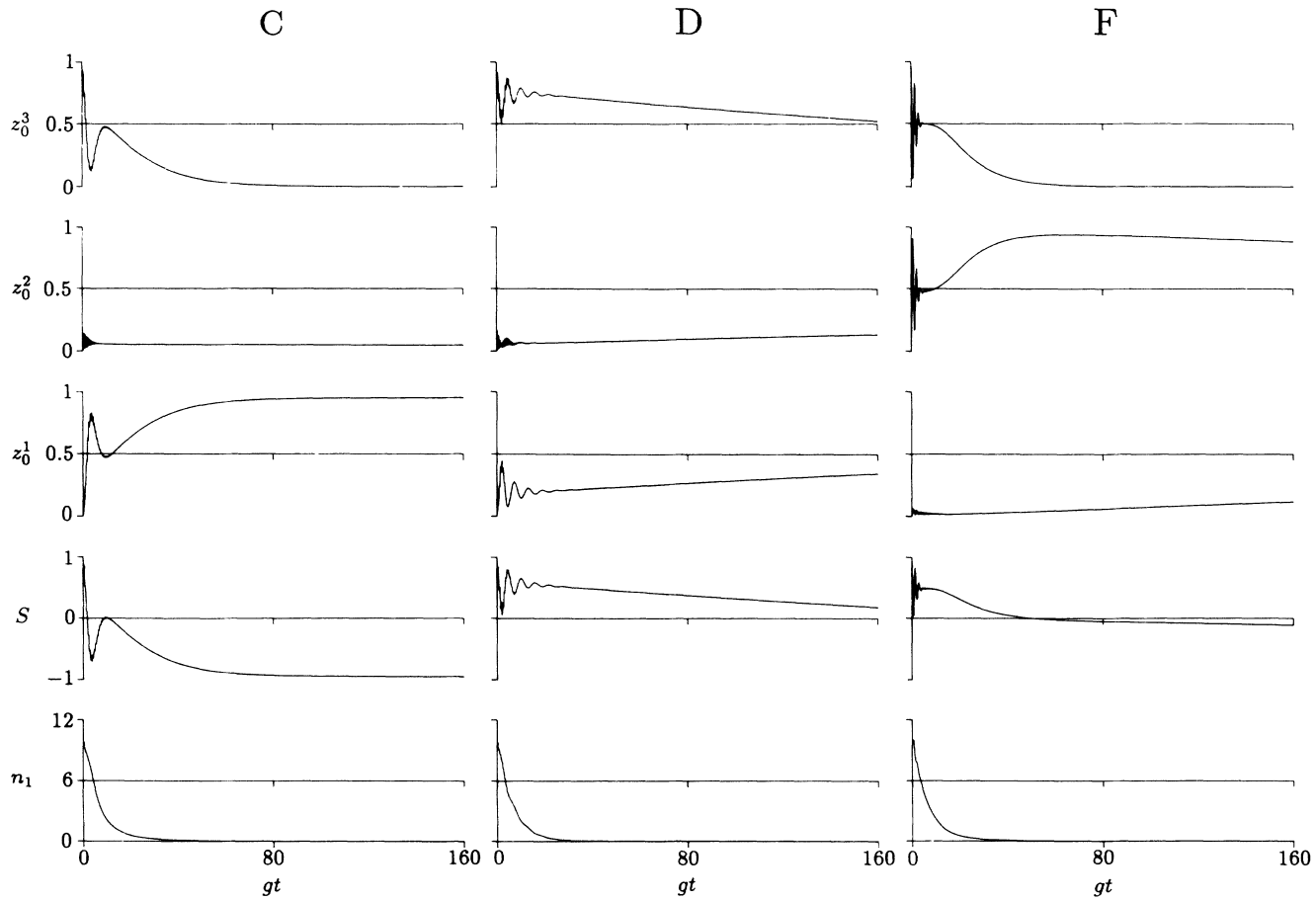

FIG. 4. Same as Fig. 3 for a larger cavity damping: $\kappa=0.08g$.

the mean photon number.

None of the cases D–F plotted in Figs. 3–5 will be discussed in this section. These cases, namely, concern the simulation of a two-level atom (one-photon transition) by changing the detuning parameters of the two-photon transition case and will be discussed in Sec. IV. In the case of strong damping (cf. case C in Fig. 4), the cavity losses are so large that no collapse or revival phenomena may appear. As it should be, the occupation probability of the highest level 3 decays to zero, and that of level 1 increases to one with time. The intermediate level 2 plays almost no role, and its occupation probability remains zero. The mean photon number decays exponentially.

IV. SIMULATION OF THE TWO-LEVEL ATOM BY CHANGING THE CORRESPONDING DETUNING PARAMETERS

In an ideal cavity ($\kappa=0$), by letting the detuning parameter Δ_r to go to zero, the cases D–F in Fig. 5 emerge from Fig. 2, case C. In this way the one-photon transition (Fig. 5, case F) emerges from the two-photon transition (Fig. 2, case C) step by step. From Fig. 5 it can be seen that, by letting the detuning Δ_r to go to zero, the strong initial influence of the level 1 vanishes and the influence of the intermediate level 2 becomes stronger step by step. Finally, for $\Delta_r=0$, the occupation probability of the level 2 will behave quite analogously to that of the level 3. This means that we get effectively a two-level atom, since the level 1 does not play any role in the radiation process.

In the case of cavity damping, the following can be seen. In Fig. 3, cases D and F, the numerical results for small cavity damping are plotted. The comparison and Fig. 5, D and F, with Fig. 3, D and F, shows that the oscillation amplitudes of the revivals are damped, but that the form of the curves is retained. Only for the mean photon number are the cavity losses clearly visible (exponential decay). In the case of strong damping, the occupation probabilities of all levels change drastically (cf. Fig. 4, D and F). For $\Delta_r=0$, the occupation probability of level 1 is almost zero. Further, the occupation probability of level 3 decays to zero and that of level 2 increases to nearly one.

V. SECOND-ORDER CORRELATION FUNCTION OF THE RADIATION FIELD (BUNCHING AND ANTIBUNCHING)

In order to investigate the properties of the radiation field, we calculate numerically the second-order correla-

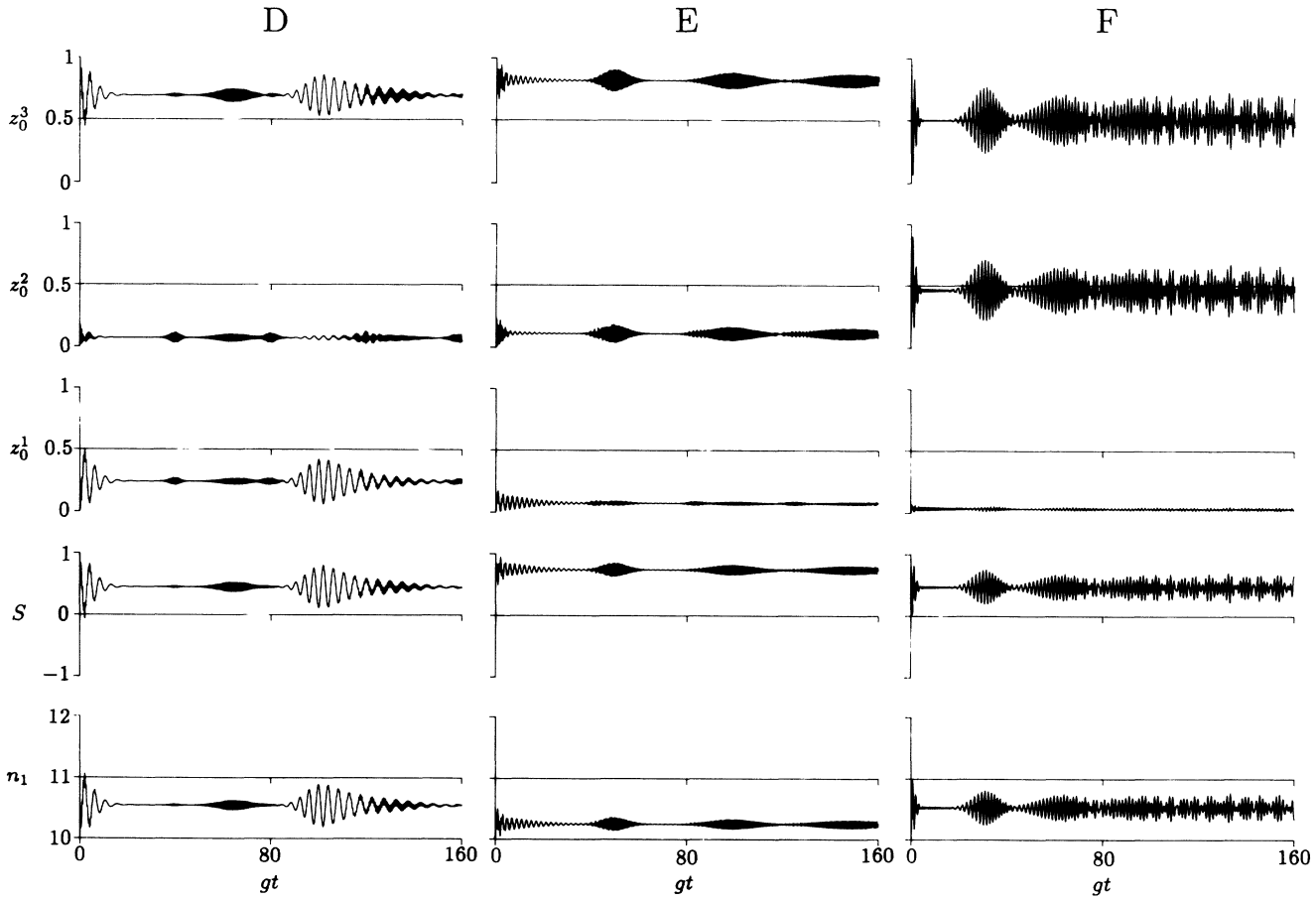

FIG. 5. Same as Fig. 2 (ideal cavity) for other detuning parameters: case D, $\Delta_l=10g$, $\Delta_r=-9g$; case E, $\Delta_l=10g$, $\Delta_r=-7g$; case F, $\Delta_l=10g$, $\Delta_r=0$.

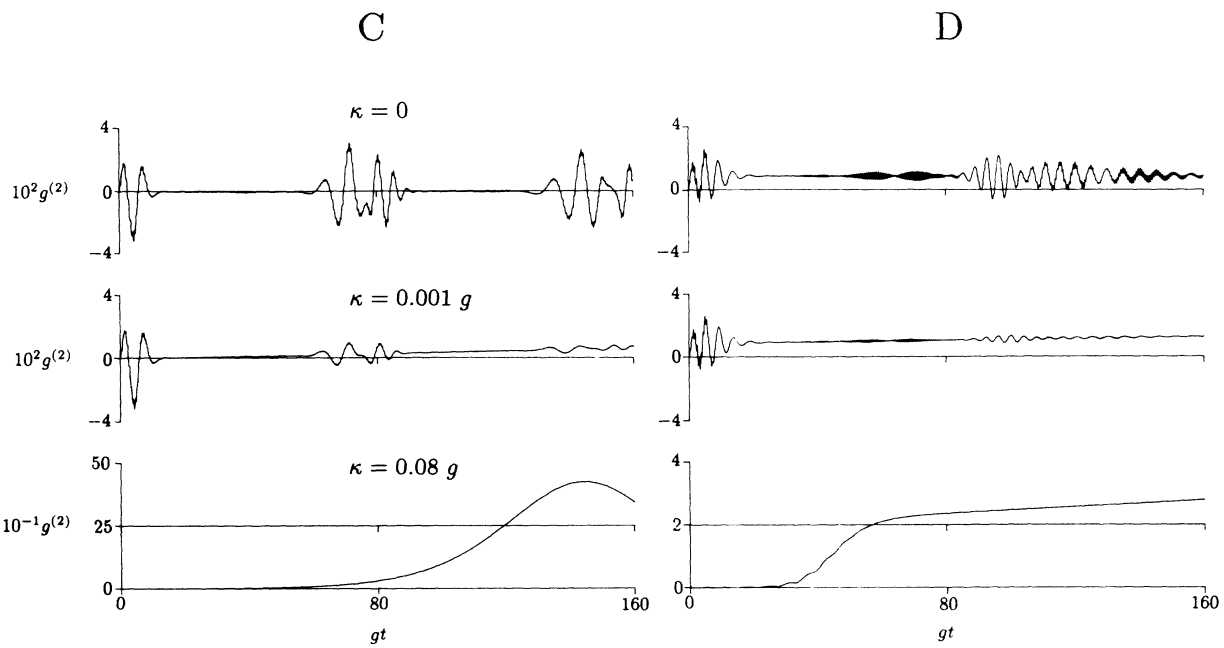

FIG. 6. The time evolution of the normalized second-order correlation function $g^{(2)}(t)$ for different cavity dampings, $\kappa=0$, $0.001g$, and $0.08g$, in the case C of the detunings, $\Delta_l=-\Delta_r=10g$, and case D, $\Delta_l=10g$, $\Delta_r=-9g$, for the same initial coherent field as in Fig. 2.

tion function:

$$g^{(2)}(t)=\frac{\langle (a^\dagger)^2a^2\rangle_t-\langle a^\dagger a\rangle_t^2}{\langle a^\dagger a\rangle_t^2}=\frac{n_2(t)}{n_1^2(t)}-1\ . \tag{29}$$

In Figs. 6 and 7, we plot $g^{(2)}(\tau)$ for different detuning (C–F) and damping parameters. In these figures the bunching and antibunching phenomena can be observed. In the undamped cases C and F ($\kappa=0$), collapses and revivals appear; whereas, in the case of collapse, $g^{(2)}(t)\approx 0$, the revival oscillations show both bunching and antibunching features. In intermediate cases D and E ($\kappa=0$), the antibunching effects almost disappear. The amplitudes of the oscillations of the revivals will be damped by small cavity losses to the extent that antibunching appears only at the very beginning of the time evolution (cf.

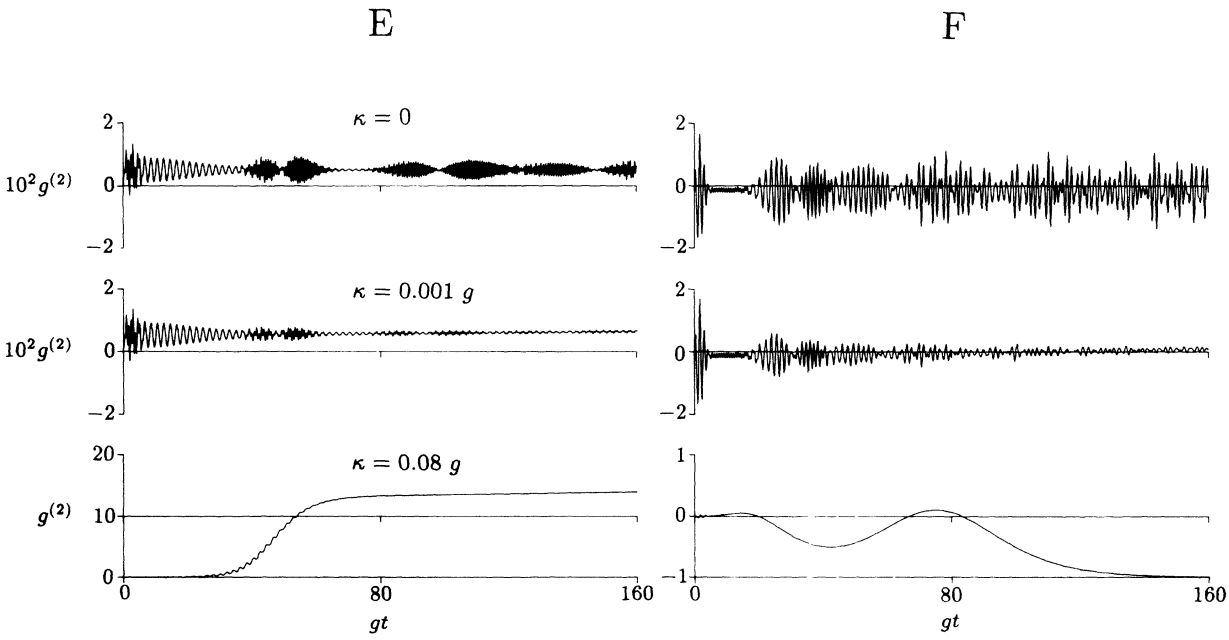

FIG. 7. Same as in Fig. 6 for the detuning parameters: case E, $\Delta_l=10g$, $\Delta_r=-7g$; case F, $\Delta_l=10g$, $\Delta_r=0$.

Fig. 6, case C, and Fig. 7, case F). In cases C, D, and E, the antibunching will disappear by increasing cavity damping ($\kappa=0.08g$).

An interesting phenomenon arises in the case of a simulated one-photon transition (case F in Fig. 7). The large damping leads to a completely antibunched radiation field in the time limit:

$$g^{(2)}(t\to\infty)=-1\ . \tag{30}$$

Of course, for $t\to\infty$, the radiation field will approach the normal vacuum.

In order to get more information about this new affect, we explore the exact two-level model as far as the antibunching is concerned. This case is examined in Fig. 8 for $\kappa=0.08g$. A comparison of this figure with Fig. 7, case F, $\kappa=0.08g$, shows that the second-order correlation function exhibits more structure in the three-level model. In both cases the same limit, Eq. (30), regarding the antibunching, will be achieved for large times. In the case of the two-level atom, this effect can be also demonstrated analytically. By use of the method developed in our previous paper,[7] it can easily be shown that the result of Eq. (30) can be obtained ($\kappa<g$) for the atom being in the excited state $|2\rangle$ and the field in the Fock state $|p\rangle$ (p is the number of photons) initially. Namely, for mean photon numbers $n_1(p,t)$ and $n_2(p,t)$, it holds that

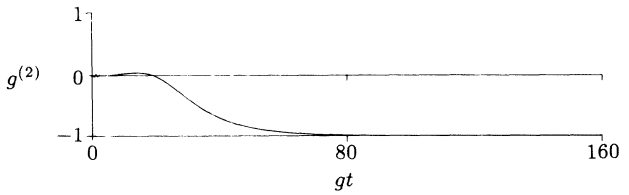

FIG. 8. The time evolution of the normalized second-order correlation function $g^{(2)}(t)$ in the case of a real two-level atom in a damped cavity ($\kappa=0.08g$) for the same initial coherent field as in the previous figures.

$$n_1(p;t)\equiv\langle 2p|a^\dagger a\exp(-itL)|2p\rangle$$
$$=\tfrac{1}{2}\begin{pmatrix}p+\frac{1}{2}\\ p\end{pmatrix}[2F(-p,-\tfrac{1}{2};\tfrac{3}{2};\exp(-2\kappa t))-F(-p,\tfrac{1}{2};\tfrac{3}{2};\exp(-2\kappa t))]\exp(-\kappa t)+\bar{n}_1(p,t),\quad p\geq 0\ , \tag{31}$$

where

$$\bar{n}_1(p,t)=-\left[\tfrac{1}{2}\cos(\beta_{p+1}gt)+\frac{1}{8(p+1)}(4p^2+5p)\frac{\kappa}{g}\beta_{p+1}\sin(\beta_{p+1}gt)\right]\exp[-(2p+1)\kappa t]$$
$$+\frac{1}{8p}(4p^2+3p+1)\frac{\kappa}{g}\beta_p\sin(\beta_p gt)\exp[-(2p-1)\kappa t],\quad p\geq 1\ ; \tag{32}$$

$$\bar{n}_1(p,t)=-\tfrac{1}{2}\cos(\beta_1 gt)\exp(-\kappa t),\quad p=0\ ; \tag{33}$$

$$\beta_p=\left[4p-\left[\frac{\kappa}{g}\right]^2\right]^{1/2}, \tag{34}$$

and

$$n_2(p;t)\equiv\langle 2p|(a^\dagger)^2a^2\exp(-itL)|2p\rangle$$
$$=\frac{1}{2}\begin{pmatrix}p+\frac{1}{2}\\ p-1\end{pmatrix}[2F(1-p,-\tfrac{1}{2};\tfrac{5}{2};\exp(-2\kappa t))-F(1-p,\tfrac{1}{2};\tfrac{5}{2};\exp(-2\kappa t))]\exp(-3\kappa t)$$
$$-\left[\tfrac{1}{2}p\cos(\beta_{p+1}gt)+\frac{1}{8(p+1)}(p-1)(4p^2+5p)\frac{\kappa}{g}\beta_{p+1}\sin(\beta_{p+1}gt)\right]\exp[-(2p+1)\kappa t]$$
$$+\frac{1}{8p}(p-1)(4p^2+3p+1)\frac{\kappa}{g}\beta_p\sin(\beta_p gt)\exp[-(2p-1)\kappa t],\quad p\geq 1\ . \tag{35}$$

By $F(\alpha,\beta;\gamma;x)$, we denoted the hypergeometric function.[10] Then, by using Eqs. (29), (31)–(35), and $F(\alpha,\beta;\gamma;0)=1$, it follows that

$$g^{(2)}(t\to\infty)=-1\ . \tag{36}$$

From this we can deduce immediately the results for the initial coherent field:

$$n_1(t)=\sum_{p=0}^{\infty}\exp(-|\alpha|^2)\frac{|\alpha|^{2p}}{p!}n_1(p,t)\ , \tag{37}$$

$$n_2(t)=\sum_{p=1}^{\infty}\exp(-|\alpha|^2)\frac{|\alpha|^{2p}}{p!}n_2(p,t)\ , \tag{38}$$

$$g^{(2)}(t\to\infty)=-1\ . \tag{39}$$

VI. CONCLUSION

In this paper we have investigated the three-level atomic model interacting with a resonant single-mode radiation field inside a cavity with arbitrary damping. We have set up exact equations of motion for the EV's of interest. These equations were solved numerically for different detunings of atomic levels. First, we detuned the intermediate level preserving the two-photon resonance ($\Delta_l = -\Delta_r$, see Fig. 1). This has the consequence that, from the cascade one-photon transitions in the tuned case, the two-photon transitions emerge if the detuning ($\Delta_l = -\Delta_r$) is increased sufficiently. In this case, as it was demonstrated in Figs. 2, 3, and 4, for case C, the one-photon transition to the intermediate level can be considered as virtual, so that the atom acts as an effective two-level system emitting (absorbing) two photons simultaneously. The small influences of the intermediate level are still visible. Just this latter fact stresses the difference between our model and that of other authors[5] who use approximative effective Hamiltonians for two-photon transitions. Of course, our results almost coincide with those of these authors in the case of large detuning of the intermediate level. Even in this case, our calculations are more general since our exact Eqs. (12)–(18) are valid for arbitrary damping; whereas those of Puri and Agarwal[5] (who use a dressed state approximation) are restricted to small-cavity damping. A simulation of the two-level atom can, of course, be achieved only in our model by decreasing the detunings of the upper levels (cf. Fig. 1 and Sec. IV).

In Sec. V we studied the normalized second-order correlation function of the radiation field. In the case of the simulated one-photon transition (Fig. 7, case F), we were able to point out the effect of total antibunching in the time limit for $t \to \infty$.

ACKNOWLEDGMENTS

The authors would like to acknowledge the useful discussions made with Professor G. S. Agarwal during his visit at their Institute. This work was supported by the Fonds zur Förderung der Wissenschaftlichen Forschung in Österreich (Vienna, Austria) under Contract No. P6690P and by the Jubiläumsfonds der Österreichischen Nationalbank zur Förderung der Forschungs- und Lehraufgaben der Wissenschaft under Contract No. 3688.

[1] H. I. Yoo and J. H. Eberly, Phys. Rep. **118**, 239 (1985).

[2] X. S. Li, D. L. Lin, and C. D. Gong, Phys. Rev. A **36**, 5209 (1987); Z. D. Liu, X. S. Li, and D. L. Lin, Phys. Rev. A **36**, 5220 (1987); D. L. Lin, X. S. Li, and Y. N. Peng, Phys. Rev. A **39**, 1933 (1989).

[3] J. M. Raimond, P. Goy, M. Gross, C. Fabre, and S. Haroche, Phys. Rev. Lett. **49**, 1924 (1982); B. Goy, J. M. Raimond, M. Gross, and S. Haroche, *ibid.* **50**, 1903 (1983); Y. Kaluzny, P. Goy, M. Gross, J. M. Raimond, and S. Haroche, *ibid.* **51**, 1175 (1983); D. Meschede, H. Walther, and G. Müller, *ibid.* **54**, 551 (1985); G. Rempe, H. Walther, and N. Klein, *ibid.* **58**, 353 (1987); J. Krause, M. O. Scully, Th. Walther, and H. Walther, Phys. Rev. A **39**, 1915 (1989).

[4] G. Adam, J. Seke, and O. Hittmair, Opt. Commun. **73**, 121 (1989).

[5] R. R. Puri and G. S. Agarwal, Phys. Rev. A **37**, 3879 (1988); R. R. Puri and R. K. Bullough, J. Opt. Soc. Am. B **5**, 2021 (1988).

[6] J. Seke, J. Opt. Soc. Am. B **2**, 1678 (1985); Phys. Rev. A **33**, 739, 4409 (1986); J. Seke, G. Adam, and O. Hittmair, Opt. Acta **33**, 703 (1986); G. Adam, J. Seke, and O. Hittmair, Z. Phys. B **65**, 527 (1987); J. Seke and F. Rattay, J. Opt. Soc. Am. B **4**, 380 (1987).

[7] G. Adam and J. Seke, Opt. Commun. **62**, 413 (1987); Nuovo Cimento **10B**, 485 (1988).

[8] J. Seke and F. Rattay, Phys. Rev. A **39**, 171 (1989).

[9] R. Bonifacio, P. Schwendimann, and F. Haake, Phys. Rev. A **4**, 302 (1971); **4**, 854 (1971).

[10] I. S. Gradshteyn and I. M. Ryzhik, *Tables of Integrals, Series, and Products* (Academic, New York, 1965), p. 1039, formula 9.100.